Pulse EPR Detection of Lipid Exchange between Protein-Rich Raft and Bulk Domains in the Membrane: Methodology Development and Its Application to Studies of Influenza Viral Membrane

Kazunori Kawasaki,* Jun-Jie Yin,† Witold K. Subczynski,‡§ James S. Hyde,‡, and Akihiro Kusumi¶‖

*National Institute of Bioscience and Human Technology, Tsukuba 305-8566, Japan; †Instrumentation and Biophysics Branch, Food and Drug Administration, Washington, DC 20204, and ‡National Biomedical EPR Center, Biophysics Research Institute, Medical College of Wisconsin, Milwaukee WI 53226 USA; §Biophysics Department, Institute of Molecular Biology, Jagiellonian University, Krakow 31-120, Poland; ¶Department of Biological Science, Graduate School of Science, Nagoya University, Nagoya 464-8602, and ‖Kusumi Membrane Organizer Project, Exploratory Research for Advancement of Technology Organization, Japan Science and Technology Cooperation, Nagoya 460-0012, Japan

ABSTRACT A pulse saturation-recovery electron paramagnetic resonance (EPR) method has been developed that allows estimation of the exchange rates of a spin-labeled lipid between the bulk domain and the protein-rich membrane domain, in which the rate of collision between the spin label and molecular oxygen is reduced (slow-oxygen transport domain, or SLOT domain). It is based on the measurements of saturation-recovery signals of a lipid spin label as a function of concentrations of both molecular oxygen and the spin label. Influenza viral membrane, one of the simplest paradigms for the study of biomembranes, showed the presence of two membrane domains with slow and fast collision rates with oxygen (a 16-fold difference) at 30°C. The outbound rate from and the inbound rate into the SLOT domain (or possibly the rate of the domain disintegration and formation) were estimated to be 7.7×10^4 and 4.6×10^4 s^{-1}, (15 μs residency time), respectively, indicating that the SLOT domain is highly dynamic and that the entire SLOT domain represents about one-third of the membrane area. Because the oxygen transport rate in the SLOT domain is a factor of two smaller than that in purple membrane, where bacteriorhodopsin is aggregated, we propose that the SLOT domain in the viral membrane is the cholesterol-rich raft domain stabilized by the trimers of hemagglutinin and/or the tetramers of neuraminidase.

INTRODUCTION

Recently, extensive attention has been paid to membrane sub-domains, in which specific lipids and proteins are assembled to carry out specific functions (Edidin, 1990; Edidin and Stroynowski, 1991; Simons and Ikonen, 1997; Mouritsen and Andersen, 1998). The size of a domain may range from a scale of several molecules (molecular clusters) up to several microns (Kusumi and Sako, 1996; Edidin, 1997; Sheets et al., 1998; Hwang et al., 1998). Data have been accumulating that indicate that many important functions of cellular membranes are closely associated with specific domains in the membrane. For example, oligomerization of immunoglobulin E-Fc receptors (i.e., formation of protein cluster domains) in the plasma membrane of basophilic leukemic cells induces membrane domains that are rich in src kinases, saturated lipids, and glycosphingolipids, which initiates the release of chemical mediators (Metzger, 1992; Thomas et al., 1994, Field et al., 1995, 1997; Torigoe et al., 1998). The subsequent Fc receptor internalization is carried out at the coated pit, a specialized domain for receptor endocytosis (Miettinen et al., 1992). Another example is the detergent-insoluble glycosphingolipid domains, which have been the subject of intensive studies in recent years (Simons and Ikonen, 1997; Brown and London, 1998; Jacobson and Dietrich, 1999). These domains may play important roles in protein sorting and signal transduction. These studies indicate that the fluid mosaic model by Singer and Nicholson (1972) has to be greatly modified to understand the structure and function of biological membranes. Therefore, molecular mechanisms by which these domain structures are formed, maintained, and disintegrated have become one of the central issues in membrane biophysics (Kusumi and Sako, 1996).

One of the critical issues in the understanding of membrane domains is the realization that these domains are not static structures, in the following two points in particular. First, the domains may be formed and disintegrated continually, with lifetimes ranging from ~10 ns for cholesterol clusters in unsaturated phosphatidylcholine (PC) membranes (Subczynski et al., 1990, 1991; Pasenkiewicz-Gierula et al., 1991), to seconds for clathrin-coated pits (Gaidarov et al., 1998), and up to hours for cell adhesion structures (Adams and Nelson, 1998). Second, even in the domains that last longer, the constituent molecules may be changing all the time. Some molecules go out whereas other molecules come in, just like micelles, in which constituent molecules move in and out continually (Simons and Ikonen, 1997).

In the present report, to simplify the presentation, we first concentrate on the second case of domain dynamism, i.e., molecular exchange between domains in the membrane, and in particular, the exchange of lipids between a domain and the bulk phase. This is the simplest case among molecular exchanges between domains and is likely to occur in a

Received for publication 17 *November* 2000 *and in final form* 22 *November* 2000.

Address reprint requests to Dr. Akihiro Kusumi, Department of Biological Science, Graduate School of Science, Nagoya University, Nagoya 464-8602, Japan. Tel.: 011-81-52-789-2969; Fax: 011-81-52-789-2968; E-mail: akusumi@bio.nagoya-u.ac.jp.

0006-3495/01/02/738/11 $2.00

variety of domains in biological membranes. We will come back to the first case in the Discussion. We have developed a new pulse electron paramagnetic resonance (EPR) spin-labeling method for detection of local domains and evaluation of lipid exchange rates. We applied this method to the study of influenza virus (IFV) membrane, one of the simplest paradigms for the study of the plasma membrane in animal cells. We found the existence of a less mobile domain, in which the oxygen diffusion-concentration product is smaller (slow-oxygen transport (SLOT) domain domain), and measured the exchange rate of a spin-labeled lipid between this domain and the bulk phase membrane.

Our method is based on variation of the local diffusion-concentration product of molecular oxygen in different membrane domains. More specifically, our method is sensitive to the product of the (local) translational diffusion coefficient and the (local) concentration of oxygen (namely, oxygen transport) in each membrane domain. Therefore, in the present paper, the word transport is used in its basic physical sense. The biological active transport across the membrane is not the subject of this paper.

Previously, Ashikawa et al. (1994) investigated a similar issue using reconstituted membranes of bacteriorhodopsin (BR) and L-α-dimyristoylphosphatidylcholine (DMPC). Using circular dichroism (CD) spectra and decay of polarized-flash-induced photodichroism of BR, they found that BR molecules are monomers in reconstituted membranes with a lipid/BR molar ratio of 80 (80-rec) and are 25% monomers and 75% trimers plus oligomers of trimers when the lipid/BR ratio is 40 (40-rec).

In the 80-rec, where the bulk domain and the boundary region around BR molecules coexist (but where no BR clusters exist), the lipid environment examined with spin-labeled lipids using pulsed saturation-recovery EPR is homogeneous on a 0.3–30-μs scale, irrespective of the presence of molecular oxygen up to 50% of atmospheric air. This is probably because the exchange rate of lipids between the bulk and the boundary regions is much greater than this time range, which is consistent with the previous results (East et al., 1985; Ryba et al., 1987, Horváth et al., 1988; Marsh, 1997). This result clearly indicates that the oxygen collision rate cannot differentiate the bulk and protein-boundary regions. Therefore, in the following, we indicate the bulk-plus-boundary regions as the BULK domain for simplicity.

In the 40-rec, two-exponential saturation-recovery EPR signals were observed in the presence of molecular oxygen (the fast recoveries that occur within 50 ns after the saturating microwave pulse due to nitrogen nuclear flip rates, etc. are neglected in the present discussion). The two time constants were close to the T_1 values in the 80-rec and those in purple membrane, where BR is aggregated. Both time constants showed linear relationships with oxygen concentration in the sample. These results can be explained by a model in which two lipid environments, possessing different oxygen transport rates with a slow exchange rate of lipids between them, are present in the membrane (further details are given below). Because one of the characteristic recovery times is close to that found in the 80-rec, it is likely to represent the recovery time in the BULK region. The second slower component in the 40-rec indicates the presence of a special lipid environment with slow oxygen transport, which was termed a slow-oxygen transport (SLOT) domain. According to Ashikawa et al. (1994), it was likely to be a self-associated BR domain (or more precisely, the domain consisting of lipids in contact with two proteins and/or lipids in contact with protein and boundary lipids), in which oxygen transport is smaller by a factor of 5 than in the BULK region. In another word, the oxygen collision rate cannot differentiate the bulk and the protein-boundary domains, but it can differentiate the protein-clustered domain (or protein-rich domain) and the BULK domain.

This treatment was possible because the exchange rates of spin-labeled lipids between these two domains, the SLOT domain and the BULK domain, were much smaller than 10^5 s^{-1} (T_1^{-1} in the absence of oxygen). In the present investigation of IFV membrane, we encountered a case in which the exchange of spin-labeled lipids between two domains had to be explicitly included in the analysis, thus enabling us to obtain the lipid exchange rates between the two domains.

In the present investigation, we studied IFV envelope membrane. IFV is 80–120 nm in diameter and is surrounded by an envelope that is made of a lipid bilayer containing two major viral transmembrane glycoproteins, hemagglutinin and neuraminidase (Booy et al., 1985; Kanaseki et al., 1997). The mole fraction of (total lipid-cholesterol):cholesterol:hemagglutinin plus neuraminidase is 60:40:2 in the IFV membrane, and the molar ratio of hemagglutinin and neuraminidase is 4:1 (Klenk et al., 1972; Kawakami et al., 1981; Webster et al., 1982). IFV membranes contain high amounts of detergent-insoluble raft lipids (Scheiffele et al., 1997a), and hemagglutinin preferentially interacts with sphingolipid-cholesterol raft domains via its transmembrane domain (Scheiffele et al., 1997b; Harder et al., 1998). During the packaging process of IFV, only the viral transmembrane proteins are selectively recruited, and other host proteins are excluded. It has been shown that hemagglutinin exists as trimers (Wilson et al., 1981), and neuraminidase as tetramers (Varghese et al., 1983). Therefore, IFV provides a well defined lipid bilayer membrane containing two well studied transmembrane proteins.

Two-component saturation-recovery signals of a fatty acid spin label incorporated in the IFV membrane were observed, indicating the presence of the SLOT domain. We think that this is the first case where the SLOT domain was found in biological membranes.

However, the recovery rate did not increase in proportion to the partial pressure of oxygen (cf. Fig. 4), which suggested the presence of another pathway that modified electron spin relaxation. Because the only pathway that we previously did not include in the relaxation scheme of the two-site relaxation was the exchange between the two sites, we thought the missing pathway was likely to be the physical exchange of lipids between the two domains. Therefore, in the present

study, exchange of lipids between the SLOT domain and the BULK domain is included in the relaxation scheme; i.e., we first develop a theory that can deal with saturation recovery in the presence of two domains with different oxygen transport rates and also lipid exchange between them. In the second part, we use the theory to obtain characteristics of the SLOT domain and the lipid exchange rates between the SLOT domain and the BULK domain.

Outline of theory

Our method is based on variations of the product of local diffusion coefficient and local concentration of molecular oxygen in various membrane domains, called the method of discrimination by oxygen transport (DOT method) by Ashikawa et al. (1994). Previously, our group has estimated oxygen transport in simple lipid membranes on the basis of the collision rate between molecular oxygen (a fast-relaxing species) and lipid-type spin labels (a slow-relaxing species) placed at specific locations in the membrane. The collision rate was monitored by measuring the spin-lattice relaxation times (T_1) of the nitroxide spin labels in the presence and absence of oxygen using a saturation-recovery technique (Kusumi et al., 1982; Subczynski et al., 1989). The local oxygen transport parameter ($2P$) at a locus x in the membrane has been defined as

$$2P(x) = T_1^{-1}(x, \text{air}) - T_1^{-1}(x, N_2) \tag{1}$$

where $2P(x)$ is proportional to the rate of collision between the spin label and molecular oxygen and is thus proportional to the product of the local oxygen concentration $[O_2(x)]$ and the local translational diffusion coefficient of oxygen $D_{O(x)}$ (thus called transport parameter) in a membrane that is in equilibrium with atmospheric oxygen:

$$2P(x) = AD_O(x)[O_2(x)], \quad A = 8\pi pr_0, \tag{2}$$

where r_0 is the interaction distance between oxygen and the nitroxide radical spin labels (~4.5 Å; Windrem and Plachy, 1980), and p is the probability that an observable event occurs when a collision does occur (A is remarkably independent of the hydrophobicity and viscosity of the solvent, and of the spin label species) and is very close to 1 (Hyde and Subczynski, 1984, 1989; Subczynski and Hyde, 1984). Previously, we used $W(x)$ rather than $2P(x)$. However, in the present report, we use several different W values, and we changed the notation for the oxygen transport parameter to avoid confusion. Note that $2P(x)$ is a value extrapolated to a sample equilibrated with 100% air, and that $[O_2(x)]$ is proportional to the partial pressure of molecular oxygen in the equilibrating gas mixture. Because, in actual experiments, nitrogen gas and dried air are mixed, we use the fraction of air in the gas mixture f_{air}.

Consider a membrane consisting of two lipid environments that can be differentiated by the difference in the rate of oxygen transport in each domain, for example, the BULK domain and the SLOT domain in the BR 40-rec membranes (Ashikawa et al., 1994). When the exchange rates of the spin-labeled lipid between these domains are slow compared with $10^5\ s^{-1}$, the saturation-recovery signal is expected to be simply a double-exponential curve with time constants of $T_1^{-1}(f_{air}, \text{SLOT})$ and $T_1^{-1}(f_{air}, \text{BULK})$, where

$$T_1^{-1}(f_{air}, \text{SLOT}) = 2P_1 f_{air} + T_1^{-1}(N_2, \text{SLOT}) \tag{3}$$

$$T_1^{-1}(f_{air}, \text{BULK}) = 2P_2 f_{air} + T_1^{-1}(N_2, \text{BULK}). \tag{4}$$

SLOT and BULK refer to the two membrane domains (x has been changed to these domains, and, in addition, the depth in the membrane is fixed for 14-doxyl eicosanoic acid spin label (14-EASL)), and f_{air} is the fraction of air in the equilibrating gas mixture. $2P_1$ and $2P_2$ are oxygen transport parameters in each domain. Because these $2P$ values are the rates of collision between the spin label and molecular oxygen extrapolated to a sample equilibrated with 100% air, $2Pf_{air}$ represents the collision rate in a sample equilibrated with a gas containing f_{air}. In the case of the 40-rec with 12-PC spin label at 30°C (Ashikawa et al., 1994),

$$T_1^{-1}(N_2, \text{SLOT}) = 0.25 \times 10^6\ s^{-1} = T_1^{-1}(N_2, \text{BULK})$$

$$2P_1 = 0.45 \times 10^6\ s^{-1}, \quad \text{and} \quad 2P_2 = 2.4 \times 10^6\ s^{-1}.$$

In the following, the above equations are expressed using electron spin transition rates; i.e.,

$$W_{10} = 1/2 \times T_1^{-1}(N_2, \text{SLOT}), \tag{5}$$

$$W_{20} = 1/2 \times T_1^{-1}(N_2, \text{BULK})$$

$$W_1 = 1/2 \times T_1^{-1}(f_{air}, \text{SLOT}), \tag{6}$$

$$W_2 = 1/2 \times T_1^{-1}(f_{air}, \text{BULK})$$

$$W_1 = P_1 f_{air} + W_{10} \tag{7}$$

$$W_2 = P_2 f_{air} + W_{20}. \tag{8}$$

In general, W_{10} and W_{20} are close in the membrane (as shown above, $T_1^{-1}(N_2, \text{SLOT}) \approx T_1^{-1}(N_2, \text{BULK})$), and the presence of two types of lipid domains can often be clearly manifested only after introducing molecular oxygen in the sample (DOT method); the collision rates of molecular oxygen with the nitroxide group of the spin label can be quite different in the two domains, and the effect of oxygen collision on the electron transition rate is generally much greater than motional effects (Kusumi et al., 1982).

In the present study, a theory has been developed to include exchange of lipid-type spin labels between two domains that possess different oxygen transport rates. The saturation-recovery signal of lipid-type spin labels intercalated in two coexisting lipid domains in the membrane was analyzed on the basis of the scheme shown in Fig. 1. Three relaxation processes are involved in saturation recoveries of spin labels exchanging between the two sites. First is electron spin-lattice relaxation at each domain; the relaxation

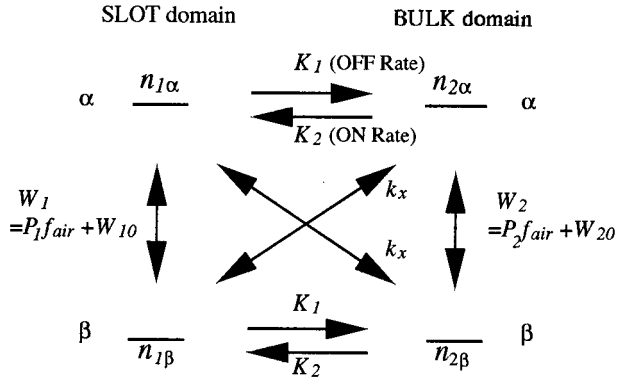

FIGURE 1 A scheme for analyzing saturation-recovery signals of spin labels in the presence of two domains that possess different oxygen transport rates: SLOT domain and the BULK (bulk plus boundary) domain. An important point in this scheme is that it includes exchanges of lipid-type spin labels between the two domains (K_1 and K_2, outbound and inbound rates of the SLOT domain, respectively; see the third and fourth terms in Eqs. 9–12). We assume that all spin label molecules are available for the exchange processes. In addition, this scheme includes the following two relaxation processes. 1) Electron spin transition of the spin label in each domain (Eqs. 5–8); the transition rates, W_1 and W_2, are linear functions of the partial pressure of air f_{air} in the equilibrating gas mixture, W_{10} and W_{20} are the electron spin transition rates at $f_{air} = 0$, and $2P_1$ and $2P_2$ are the rates of oxygen collision with the spin label in a sample equilibrated with air (see the first and second terms in Eqs. 9–12). 2) Heisenberg exchange between the spins in different domains (k_x is the Heisenberg exchange rate; see the fifth and sixth terms in Eqs. 9–12). The three states of the doxyl nitrogen nuclear spin are assumed to mix into a single state because of fast nuclear spin relaxation.

rates, W_1 and W_2, are linear functions of f_{air} as described in Eqs. 5–8, and W_{10} and W_{20} are the electron spin-lattice relaxation rates at $f_{air} = 0$. Second is physical exchange of lipids between the two domains (K_1 and K_2 are the exchange rates). We assume that all spin label molecules are available for the exchange reaction; i.e., the domains must be small for this formalism to be valid. We will come back to this point in the Discussion. Third is Heisenberg exchange between the spins in different domains (k_x is the Heisenberg exchange rate). Experiments with high as well as low concentrations of spin probes were necessary because the first and second are not sufficient to determine six unknown parameters (W_{10}, P_1, W_{20}, P_2, K_1, and K_2; see Eqs. 7–20).

In this scheme, the three states of the doxyl nitrogen nuclear spin are assumed to mix into a single state because of fast nuclear spin relaxation (thus, the Heisenberg exchange rate within a domain is masked). We have measured the transition rate (W_N) of the doxyl nitrogen of 16-doxyl stearic acid spin label (16-SASL) in DMPC membranes above the phase transition temperature for the fast motional domain and that of 5-SASL in DMPC membranes below the phase transition temperature for the slow motional domain (molar ratio of SASL/DMPC = 1/400) by using electron-electron double-resonance techniques (Popp and Hyde, 1982). In the temperature range between 5 and 37°C, W_N was greater than $1/2T_1$ by a factor between 7 and 30. 12-SASL in dielaidoyl-PC membrane showed that W_N was greater than $1/2T_1$ by a factor of 34 above the phase transition temperature (37°C). These results indicate that nuclear relaxation of the doxyl nitrogen is sufficiently fast to allow the above assumption that the three nuclear states are mixed into a single nuclear state (see also Yin et al., 1987). Therefore, Heisenberg exchange within a domain was not considered here.

Yin et al. (1987) previously studied a spin relaxation problem with a similar mathematical formalism. They studied the collision rate between ^{14}N and ^{15}N spin probes. Due to the fast relaxation of each nuclear spin, only two electron spin states had to be considered for ^{14}N and for ^{15}N spin probes. Because the nuclear spin relaxation rates are substantially greater than the rate of Heisenberg exchange, which is induced by the collision of spin probes, collision of spin probes of the same nuclear species did not contribute to relaxation processes. The only meaningful collisions for the electron spin relaxation in the system are those inducing the Heisenberg exchange between ^{14}N and ^{15}N spin probes.

Following Yin et al. (1987), a set of rate equations can be set up as follows:

$$\frac{dn_{1\alpha}}{dt} = -W_1(n_{1\alpha} - N_{1\alpha}) + W_1(n_{1\beta} - N_{1\beta}) - K_1 n_{1\alpha} + K_2 n_{2\alpha} - k_x n_{1\alpha} n_{2\beta} + k_x n_{1\beta} n_{2\alpha} \quad (9)$$

$$\frac{dn_{1\beta}}{dt} = -W_1(n_{1\beta} - N_{1\beta}) + W_1(n_{1\alpha} - N_{1\alpha}) - K_1 n_{1\beta} + K_2 n_{2\beta} - k_x n_{1\beta} n_{2\alpha} + k_x n_{1\alpha} n_{2\beta} \quad (10)$$

$$\frac{dn_{2\alpha}}{dt} = -W_2(n_{2\alpha} - N_{2\alpha}) + W_2(n_{2\beta} - N_{2\beta}) - K_2 n_{2\alpha} + K_1 n_{1\alpha} - k_x n_{2\alpha} n_{1\beta} + k_x n_{2\beta} n_{1\alpha} \quad (11)$$

$$\frac{dn_{2\beta}}{dt} = -W_2(n_{2\beta} - N_{2\beta}) + W_2(n_{2\alpha} - N_{2\alpha}) - K_2 n_{2\beta} + K_1 n_{1\beta} - k_x n_{2\beta} n_{1\alpha} + k_x n_{2\alpha} n_{1\beta}, \quad (12)$$

where n values represent the instantaneous spin populations per unit volume of the four levels, and N values represent the equilibrium Boltzmann populations per unit volume of the four levels.

The solution to Eqs. 9 - 12 is (Yin et al., 1987)

$$I(t, f_{air}, N) = I_1[1 - \exp\{-(A - B)t\}] + I_2[1 - \exp\{-(A + B)t\}] \quad (13)$$

$$A(f_{air}, N) = W_1 + W_2 + (1/2)(K_1 + K_2 + k_x N) \quad (14)$$

$$B(f_{air}, N) = [(W_1 - W_2)^2 + (W_1 - W_2)\{K_1 - K_2 + (K_1 - K_2)k_x N/(K_1 + K_2)\} + (1/4)(K_1 + K_2 + k_x N)^2]^{1/2} \quad (15)$$

$$N = n_{1\alpha} + n_{1\beta} + n_{2\alpha} + n_{2\beta}, \quad (16)$$

where $I(t, f_{air}, N)$ is the observed saturation-recovery signal, I_1 and I_2 are constants to be defined by initial conditions, and N represents the total number of spins per unit volume and is proportional to the number of spin probes incorporated in the membrane.

As discussed below, all the rate constants (W_{10}, P_1, W_{20}, P_2, K_1, K_2, and k_x) were determined by obtaining saturation-recovery signals at various partial pressures of oxygen (at low spin-label concentrations), and at various concentrations of the spin label without oxygen. Dependencies of A and B^2 on oxygen concentration can be determined by the following equations obtained from Eqs. 7, 8, 14, and 15 (assuming $N = 0$, i.e., for a low concentration of the spin label):

$$A(f_{air}) = (P_1 + P_2)f_{air} + W_{10} + W_{20} + (1/2)(K_1 + K_2) \quad (17)$$

$$B(f_{air})^2 = (P_1 - P_2)^2 f_{air}^2 + (P_1 - P_2)[2(W_{10} - W_{20}) + (K_1 - K_2)]f_{air} + (W_{10} - W_{20})^2 + (W_{10} - W_{20})(K_1 - K_2) + (1/4)(K_1 + K_2)^2 \quad (18)$$

Dependencies of A and $(A - B)(A + B)$ on the spin label concentration, N, in the absence of oxygen ($f_{air} = 0$) can be obtained from

$$A(N) = (1/2)k_x N + W_{10} + W_{20} + (1/2)(K_1 + K_2) \quad (19)$$

$$(A(N) - B(N))(A(N) + B(N)) = [W_{10} + W_{20}(W_{10} - W_{20})(K_1 - K_2)/(K_1 + K_2)]k_x N + 4W_{10}W_{20} + 2W_{10}K_2 + 2W_{20}K_1. \quad (20)$$

All coefficients on the right side of Eqs. 17–20 were determined by fitting the curves of A versus f_{air}, B^2 versus f_{air}, A versus N, and $(A - B)(A + B)$ versus N. These include nine coefficients. However, the constant terms for Eqs. 17 and 19 are the same. Therefore, 8 equations are obtained by determining the coefficients in Eqs. 17–20. Because there are only seven rate constants, all of them can be determined by solving these equations for coefficients.

MATERIALS AND METHODS

The 14-EASL) was purchased from Molecular Probes (Eugene, OR). IFV was prepared as described previously (Kanaseki et al., 1997). Ethanol solutions of 14-EASL over the range of 3–100 nmol/10 μl were added to the IFV suspension (2 mg of total protein/1 ml of 5 mM PIPES and 145 mM NaCl, pH 7.5) to give final concentrations of over the range of 3–100 μM. After incubation for 30 min at 37°C, each sample was mixed with 1 ml of borate buffer (100 mM sodium borate, pH 9.5) and was centrifuged for 1 h at 130,000 $\times$ g at 4°C. The sedimented virus was resuspended in 2 ml of the borate buffer and centrifuged again.

Concentrations of 14-EASL in IFV membrane were determined in the following way. Total lipid of the IFV envelope was extracted from labeled IFV by the method of Bligh and Dyer (1959), and concentrations of 14-EASL and phospholipids were determined from the EPR signal intensity and by the phosphorous assay of Bartlett (1959), respectively.

Liposomes made of the total lipid extracted from the IFV envelope membrane that had been labeled with 3 μM 14-EASL (a mole ratio of 14-EASL/phospholipid in the IFV envelope = 0.0034) were prepared as before (Kusumi et al., 1986).

The samples for pulse EPR experiments were pelleted by centrifugation at 178,000 $\times$ g for 25 min (Airfuge, Beckman, Palo Alto, CA), and the pellet was placed in a gas-permeable capillary (inner diameter, 0.6 mm) made from the methylpentene polymer called TPX for EPR measurements. The concentration of oxygen in the sample was controlled by equilibrating the sample with the same gas that was used for temperature control, a mixture of nitrogen and dry air (Kusumi et al., 1982).

Saturation-recovery pulse EPR measurements were performed as described previously with the use of a loop-gap resonator (Kusumi et al., 1982; Yin et al., 1987; Subczynski et al., 1989). The microwave field for short pulse experiments was in the range of 2.0 and 3.5 G (1 G = 10^{-4} T), and the pulse length in the range of 0.1–0.5 μs (Yin et al., 1987, 1988, 1990). Typically 10^4-10^5 decays/s were acquired with 512 data points on each decay. The total accumulation time was typically 5–20 min. Saturation-recovery curves were analyzed for double-exponential decays using a curve-fitting program based on the Monte Carlo method (improved from the program by Yin et al., 1987). A least-squares minimization function was used as the criterion of excellence of the fit between the model and experiment.

The experiments were repeated at least seven times for each point (IFV separately prepared three times). All these data points were used to obtain the best-fit parameters by the curve fitting (Figs. 5 and 6). When the best-fit parameters were obtained for each of the three independent experiments (using independently prepared virus), the nine coefficients in Eqs. 17–20 and the relaxation parameters in Table 2 were different by ±20% except for the second term in Eq. 18 (±42%) and K_1 (±32%).

RESULTS

Fig. 2 shows the conventional EPR spectrum of 14-EASL in the membrane of IFV at 30°C, suggesting the presence of at least two lipid environments with different levels of restriction on motion of alkyl chains (Knowles et al., 1979; Marsh et al., 1982). The use of the spin probe attached to the C14 of the acyl chain was first employed by Knowles et al. (1979). Their results indicated that the presence of two components in a spectrum is visually more clear with phospholipids labeled at the C14 than at other positions in the

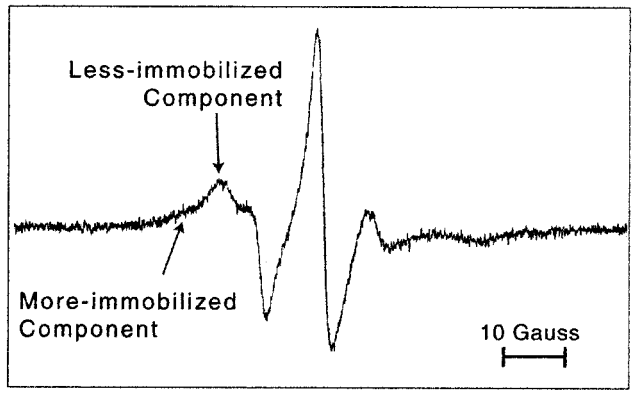

FIGURE 2 Conventional EPR spectrum of 14-EASL in the membrane of IFV at 30°C, suggesting the presence of at least two lipid environments with different levels of restriction on motion of alkyl chains.

alkyl chain. The more immobile component (the outer peak in the low-field line) is likely to represent the lipid in the boundary region of membrane proteins. In addition to the boundary component, as shown later in the case of IFV membrane, this component is likely to represent the SLOT domain (i.e., the more immobile component is likely to include both the boundary and the SLOT domain).

In Fig. 3, saturation-recovery curves are shown as a function of oxygen concentration in the equilibrating gas mixture (low concentration of the spin probe, i.e., the molar ratio of 14-EASL/phospholipid = 0.34%; Fig. 3 *A*) and of the spin label concentration in the sample (without molecular oxygen; Fig. 3 *B*). As the concentrations of oxygen or the spin label were increased, the recovery became faster.

The two characteristic time constants for the recovery ($A - B$ and $A + B$ in Eq. 13) observed in the low concentration of 14-EASL (0.34 mol % against phospholipid) are plotted in Fig. 4. If there was no exchange of spin-labeled lipids between the two domains and no Heisenberg exchange, $A - B = 2W_1$ and $A + B = 2W_2$, both of which have a linear relationship with f_{air}. This was the case found in the 40-rec of BR by Ashikawa et al. (1994), where the recovery time constants directly represent W_2 and W_1, the electron spin-lattice relaxation rates in the BULK and BR-aggregated domains, respectively. However, as

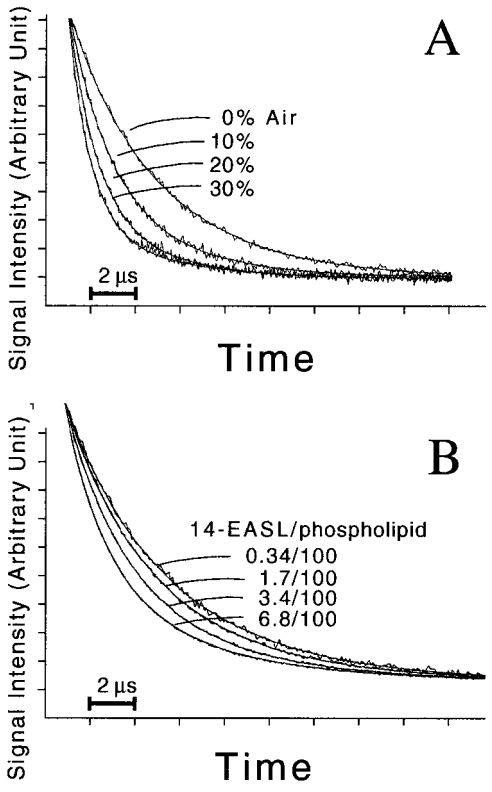

FIGURE 3 Saturation-recovery signals and fitted curves shown as a function of f_{air} (low concentration of the spin probe, i.e., 0.34 mol % 14-EASL/phospholipid; *A*) and of the spin label concentration in the sample (without molecular oxygen; *B*). As the concentrations of oxygen or the spin label were increased, the recovery became faster.

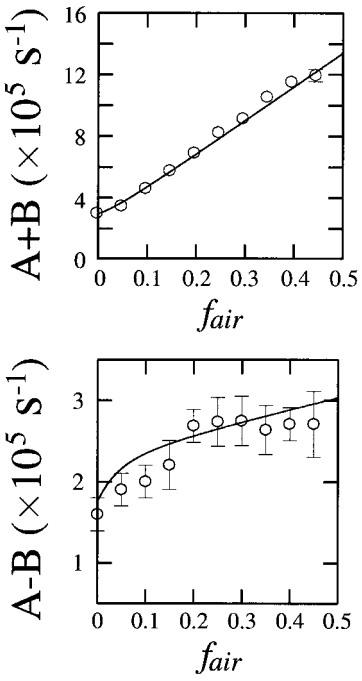

FIGURE 4 The two characteristic time constants for the recovery ($A - B$ and $A + B$ in Eq. 13) observed in the low concentration of 14-EASL (0.34 mol % against total phospholipid) plotted as a function of f_{air}. The solid curves show the values calculated from the determined kinetic constants (see the text at the end of Results). The data shown are those obtained from all the experiments (seven measurements), and the error bar indicates the standard error. The points that do not show error bars are those where error bars are smaller than the keys.

can be seen in the plots, neither $A + B$ nor $A - B$ in the IFV membrane is linear with f_{air} (The nonlinearity is clearer with $A - B$). This result suggests the presence of competing pathways for electron spin-lattice relaxation, a major one of which, we thought, is likely to be the physical exchange of lipids between the two domains.

The parameters A (Eq. 17) and B^2 (Eq. 18) are plotted against f_{air} in Fig. 5 ($N \approx 0$). In Fig. 6, A (Eq. 19) and $A^2 - B^2$ (Eq. 20) are plotted against the spin label concentrations in the medium to label IFV ($f_{air} = 0$). Actual concentrations of 14-EASL in IFV membrane expressed as the molar ratio of 14-EASL versus phospholipid in the envelope membrane were determined as described in Materials and Methods. It was found that the ratio was proportional to the amount of added label under our experimental conditions (in the range of 3–100 μM used): the ratio of 14-EASL/phospholipid = $1.13 \times C/1000$, where C is the concentration of the label in the incubation mixture expressed in micromolar concentration. Heisenberg exchange is likely to occur at the domain boundaries, and this suggests that the size of each SLOT domain is small.

The coefficient of each term in Eqs. 17–20 was determined by performing curve fitting as shown in Figs. 5 and 6 and are listed in Table 1. As described above, determination of these fitting coefficients provide eight independent

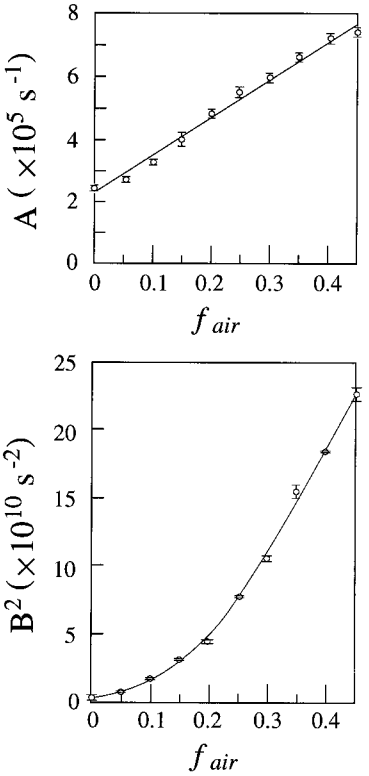

FIGURE 5 The parameters A and B^2 plotted against f_{air} (Eqs. 17 and 18). The solid curves indicate the fitted curves based on these equations. The coefficient of each term in Eqs. 17 and 18 was determined by the curve fitting (see the first five lines in Table 1 for determined coefficients). The data shown are those obtained from all the experiments (seven measurements), and the error bars indicate standard errors.

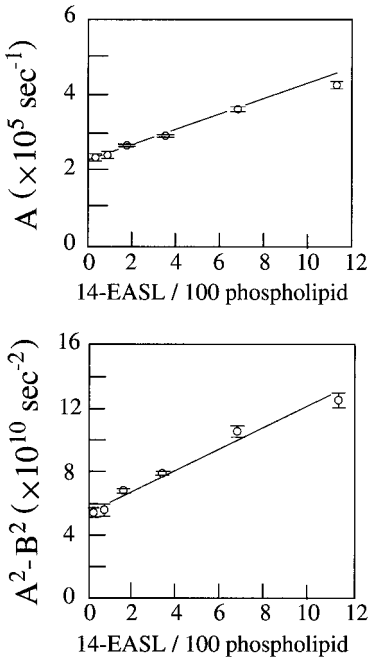

FIGURE 6 A and $A^2 - B^2$ plotted against the spin label concentration N (expressed as the mole fraction against the total phospholipid in the IFV membrane) in the medium to label IFV. The solid curves show the results of fitting based on Eqs. 19 and 20. The coefficient of each term in Eqs. 19 and 20 was determined by the curve fitting (see the last four lines in Table 1 for determined coefficients). The data shown are those obtained from all the experiments (seven measurements), and the error bars indicate standard errors.

equations (the constant terms in Eqs. 17 and 19 are the same, and experimentally similar values were obtained as shown in Table 1). Therefore, all seven rate constants can be obtained, which are summarized in Table 2. In these calculations, the constant term in Eq. 20 was not used. However, W_{10}, W_{20}, K_1, and K_2 determined from other coefficients are consistent with the constant term in Eq. 20.

In Fig. 4, the two saturation-recovery time constants $A + B$ and $A - B$ are plotted against f_{air}. The solid lines represent calculated values for $A + B$ and $A - B$ based on the kinetic constants determined as described above. If there had been no exchange, as was the case with the BR 40-rec membranes, these time constants would have represented the electron spin-lattice relaxation rate in each domain. The agreement between the measured values and the calculated curves indicate that the method developed here is useful in analyzing the saturation-recovery data on biological membranes where the SLOT domains exist and the rates of the lipid exchange between the SLOT domain and the BULK domain become comparable to the nitroxide T_1^{-1}.

To examine the effect of the presence of transmembrane proteins, i.e., hemagglutinin and neuraminidase, on the electron spin transition rate and the oxygen transport parameter, these relaxation parameters were measured for liposomes made of the total lipid extracted from the IFV membrane, and are shown in Table 2. Oxygen transport parameters in the SLOT and BULK domains are smaller than that in total lipid liposomes by a factor of 36 and 2.3, respectively, indicating a large decrease in the SLOT domain.

DISCUSSION

The SLOT domain in the IFV membrane is likely to be a protein-rich, cholesterol-containing raft domain

The oxygen transport rate in the SLOT domain, $2P_1$, is smaller than that in purple membrane, where BR molecules are aggregated, by a factor more than two (see Tables 2 and 3). It is smaller than $2P_2$, the oxygen transport rate in the BULK domain, by a factor of 16 ($2P_1/2P_2 = 0.14/2.2 = 1/16$, both numbers from Table 2), which is a large factor. This factor is even a factor of about two greater than the difference in oxygen transport parameter between DMPC membranes in the fluid phase and purple membrane (see Table 3, indicating purple membrane/DMPC for 12-PC = 0.40/3.2 = 1/8; Ashikawa et al., 1994). These comparisons suggest a possibility that the SLOT domain in the influenza viral membrane may not simply be a protein-rich region, but

TABLE 1 Evaluation of coefficients of Eqs. 17–20 at 30°C

Eq.	Coefficients	Measured value
17	$P_1 + P_2$	$1.19 \times 10^6\ s^{-1}$
17	$W_{10} + W_{20} + (1/2)(K_1 + K_2)$	$2.31 \times 10^5\ s^{-1}$
18	$(P_1 - P_2)^2$	$1.10 \times 10^{12}\ s^{-2}$
18	$(P_1 - P_2)[2(W_{10} - W_{20}) + (K_1 - K_2)]$	$2.05 \times 10^{10}\ s^{-2}$
18	$(W_{10} - W_{20})^2 + (W_{10} - W_{20})(K_1 - K_2) + (1/4)(K_1 + K_2)^2$	$3.13 \times 10^9\ s^{-2}$
19	$(1/2)k_x$	$2.10 \times 10^3\ s^{-1}$*
19	$W_{10} + W_{20} + (1/2)(K_1 + K_2)$	$2.36 \times 10^5\ s^{-1}$
20	$[W_{10} + W_{20} - (W_{10} - W_{20})(K_1 - K_2)/(K_1 + K_2)]k_x$	$7.66 \times 10^8\ s^{-2}$*
20	$4W_{10}W_{20} + 2W_{10}K_2 + 2W_{20}K_1$	$5.38 \times 10^{10}\ s^{-2}$

When the best-fit parameters were obtained for each of the three independent experiments (using independently prepared virus), the accuracies of these coefficients were better than ±20% except for the second term in Eq. 18 (±42%).

*These values are normalized to a 14-EASL/phospholipid mole ratio of 0.34% in the IFV membrane. This concentration is close to the standard spin label/phospholipid mole ratio of 1/300, which we employ for pulse EPR measurements of liposomes.

a cholesterol-rich as well as protein-rich domain because cholesterol can further reduce the oxygen collision rate (see Table 4) (Subczynski et al., 1989, 1991; Pasenkiewicz-Gierula et al., 1991; also see Subczynski et al., 1990, 1994). The mole fraction of (total lipid-cholesterol):cholesterol: hemagglutinin-plus-neuraminidase is 60:40:2 in the IFV membrane (Klenk et al., 1972; Kawakami et al., 1981; Webster et al., 1982).

The SLOT domain must be rich in the trimers of hemagglutinin and/or tetramers of neuraminidase. These are the major protein components in the IFV membrane, and hemagglutinin and neuraminidase represent ~80% and 20% of membrane proteins, respectively (Webster et al., 1982). Hemagglutinin exists as trimers (Wilson et al., 1981), whereas neuraminidase exists as tetramers (Varghese et al., 1983). They are both transmembrane proteins with a single transmembrane α-helix. In the lipid regions corralled by three and/or four α-helices, the oxygen transport rate would be greatly reduced because the transport rate within rhodopsin (protein itself), which consists of seven α-helices, is smaller than that in DMPC membranes in the liquid-crystalline state by a factor of ~100 (Subczynski et al., 1992).

We do not think that the SLOT domain is a simple raft domain consisting of cholesterol, glycosphingolipids, and glycosylphosphatidylinositol-anchored proteins. Because the oxygen transport rate in the SLOT domain is much smaller than that expected for cholesterol-rich domains (see Table 4 and compare DMPC with and without cholesterol) (Subczynski et al., 1989, 1991) or the domains containing single (nonassociated) transmembrane α-helices (see Table 4 and compare POPC with and without the peptide) (Subczynski et al., 1998), the presence of clustered transmembrane proteins in the domain is essential to explain the slow rate of oxygen transport in the domain (Ashikawa et al., 1994). Furthermore, as stated above, the oxygen transport rate in the SLOT domain is even smaller than that in purple membrane (Table 3) (Ashikawa et al., 1994). Based on these results, we propose that the SLOT domain in the IFV membrane may be a raft domain that is rich in cholesterol and stabilized by the presence of clustered proteins.

In addition, it has been shown that hemagglutinin preferentially partitions into the raft domain (Harder et al., 1998; Scheiffele et al., 1997a), which is consistent with the above model. Ge et al. (1999) characterized the liquid-ordered phase of detergent-resistant membranes from rat basophilic leukemia 2H3 cells by an EPR spin-labeling technique and concluded that biological membranes containing high concentrations of cholesterol are likely to contain a liquid-ordered phase.

The exchange rates from and to the SLOT domain were estimated to be 7.7 and $4.6 \times 10^4\ s^{-1}$, respectively (Table 2). These values are a factor of ~300 smaller than the exchange rate of lipids between the bulk domain and the boundary regions around transmembrane proteins (East et al., 1985; Ryba et al., 1987, Horváth et al., 1988; Marsh, 1997). This result indicates that the residency time of lipids in the SLOT domain is substantially longer than in the boundary region and suggests that the SLOT domain may play important roles in the function of the plasma membrane. The SLOT domain may be important in packaging the IFV membrane proteins during the budding process and in increasing the probability of successful fusion events by concentrating hemagglutinin in the SLOT domain.

In the present theoretical model, all spin probes in a domain are assumed to be available for physical exchanges and Heisenberg exchanges with probes in the other domain; i.e., the domains are small. The agreement between the theory and experiments suggests that this assumption is largely correct. Assuming that diffusion coefficients of lipids in the SLOT domain and the BULK domain are 10^{-10} and $10^{-8}\ cm^2\ s^{-1}$, respectively (see Table 1 in Lee et al., 1993; Table 1 in Sheets et al., 1998; and Table 1 in Korlach et al., 1999), these molecules can cover areas of 1 nm^2 and 100 nm^2 over 20 μs (inverse the slowest relaxation parameter, K_2, in Table 2), respectively, corresponding to areas occupied by 2 and 200 phospholipid molecules, respectively. Therefore, each SLOT domain is likely to consist of small numbers of lipids; i.e., even a lipid molecule in the core region of the domain is only one lipid away from the BULK phase (because a lipid molecule in the SLOT domain

can cover only an area of two lipid molecules during 20 μs to be available for physical and Heisenberg exchanges). It follows then that each SLOT domain has an area of only 10–20 lipid molecules. Meanwhile, each BULK domain may contain greater numbers of lipid molecules.

In the argument advanced so far, we assumed that the exchange rates of lipids between the two domains are greater than the rates at which these (transient) domains are formed and disintegrated. However, these two processes cannot be distinguished. If the lifetime of the SLOT domain is shorter than the exchange rate, the SLOT domain becomes the BULK domain before the lipid exchange takes place. Therefore, in this case, we measure the lifetime of the SLOT domain. In addition, the size distribution of these domains cannot be estimated by the present method.

Each SLOT domain may be small in size, but the entire SLOT domain occupies substantial area in the IFV membrane. From the ratio of the inbound (K_1) versus the outbound (K_2) rates of the lipid in the SLOT domain, the SLOT domain as a whole may occupy about one-third of the membrane ($K_2/[K_1 + K_2] = 0.046/[0.077 + 0.046] = 0.37$).

The oxygen transport parameter in the BULK domain in the viral membrane, $2P_2$, is smaller than $2P$ in the total lipid liposome by a factor of 2.3 ($2P/2P_2 = 5.0/2.2$, both numbers from Table 2). In the 80-rec BR membrane, $2P$ was smaller than that of DMPC membrane by a factor of 1.6 ($2P$ for the 80-rec divided by $2P$ for the DMPC membrane = 2.0/3.2 (both numbers from Table 3) = 1/1.6), indicating that these factors (2.3 and 1.6) are comparable (Ashikawa et al., 1994). This result suggests that the BULK domain in the IFV membrane also contains hemagglutinin and/or neuraminidase, although the molar ratio of protein/lipid would be lower than that in the SLOT domain.

Finally, we would like to emphasize again that the SLOT domain, which is a protein-rich raft domain in the IFV membrane, is a dynamic structure. Either the constituent lipid molecules stay in the SLOT domain and the BULK domain for less than 20 μs (inverse of K_2, the slower exchange rate) or these domains are continually formed and dispersed at an average of every 20 μs.

TABLE 2 Evaluation of rate constants ($\times 10^6$ s^{-1}) described in Fig. 1 observed at 30°C

	IFV membrane		Liposome
	SLOT domain	BULK domain	(total lipid)
Electron spin transition rate	liteW$_{10}$ = 0.08	W_{20} = 0.095	W_0 = 0.23
Oxygen transport parameter	$2P_1$ = 0.14	$2P_2$ = 2.2	$2P$ = 5.0
Lipid exchange rate	K_1 = 0.077	K_2 = 0.046	

When the best-fit parameters were obtained for each of the three independent experiments (using independently prepared virus), the accuracies for these relaxation parameters were better than ±20% except for K_1 (±32%).

The DOT method may be useful for detecting protein-stabilized rafts and measuring the lipid exchange rate

Molecular oxygen is small in size and somewhat hydrophobic, and its transport as measured by the rate of collision with spin labels is sensitive to dynamics of lipid alkyl chains and to the free volume in the membrane. Therefore, molecular oxygen has become a unique, useful probe to investigate alkyl chain dynamics and very local properties of alkyl chain packing in membranes (Kusumi et al., 1982; Subczynski et al., 1989, 1991, 1992, 1998; Ashikawa et al., 1994).

In BR reconstituted membranes, the oxygen transport parameter detected the presence of a special lipid domain that only appears in the presence of BR trimers and oligomers of trimers (Ashikawa et al., 1994). This domain exhibited a slow oxygen transport rate, which was thus termed the SLOT domain. This domain was thought to be protein rich, in which every lipid molecule is in contact with two proteins or with a protein and boundary lipids (thus the lipids are sandwiched either between two proteins or between a protein and boundary lipids) and its alkyl chain motion is suppressed to the level of the gel-phase membrane. The lifetime of this trapped-lipid domain must be greater than the rotational relaxation time of BR trimers or oligomers of trimers, which was longer than ~100 μs (Ashikawa et al., 1994). The exchange rate of lipids between this SLOT domain and the BULK domain was not observed, and was thought to be too slow to be observed with the T_1 technique (less than 10^4 s^{-1}) (Ashikawa et al., 1994).

In the present investigation, the pulse EPR technique was applied to the study of membrane domains in the influenza viral membrane, which has a lipid composition that is similar to that of the plasma membrane of animal cells. The saturation-recovery signal was double exponential in the microsecond range even in the absence of molecular oxygen, suggesting the existence of two lipid environments. The presence of two lipid domains was more clearly shown by introducing molecular oxygen to the sample because the rates of collision between the spin label and molecular oxygen are very different in the two domains. We believe that this is the first case where a SLOT domain was found in a biological membrane.

A theory was developed to obtain exchange rates of 14-EASL between the two domains with slow and fast oxygen transport rates, which includes 1) electron spin lattice relaxation in each domain including collision with molecular oxygen, 2) physical lipid exchange between the two domains (we assume that all spin label molecules are

TABLE 3 Oxygen transport parameters ($2P \times 10^6$ s^{-1}) observed with 12-PC and 16-SASL in BR-DMPC reconstituted membranes at 30°C

Probe	DMPC	80-rec	40-rec (BULK)	40-rec (SLOT)	Purple membrane
12-PC	3.2	2.0	2.3	0.40	0.40
16-SASL	3.7	2.4	2.1	0.80	0.30

TABLE 4 Oxygen transport parameters ($2P \times 10^6$ s^{-1}) observed at 30°C in the membranes of DMPC with and without 50 mol % cholesterol and in the membranes of POPC with and without 10 mol % acetyl-$K_2L_{24}K_2$-amide, a transmembrane α-helical peptide

Probe	DMPC	DMPC + 50% cholesterol	POPC	POPC + 10% peptide
5-SASL (5-PC)	2.1	0.26	1.1	0.9
10-PC	ND	ND	1.7	1.5
16-SASL (16-PC)	3.7	3.1	2.2	2.1

available for the exchange reaction), and 3) Heisenberg exchange between the spins in different domains. Because nuclear relaxation of the doxyl nitrogen was sufficiently fast ($<10^{-7}$ s), the nuclear spin states were mixed to allow an approximation of a single state in a time scale longer than 10^{-7} s and made the Heisenberg exchange within a domain unimportant. All rate constants were determined by observing saturation-recovery signals at various oxygen and spin-label concentrations in the influenza viral membrane at 30°C. The oxygen transport parameter in the SLOT domain was smaller than that in the BULK domain by a factor of 16 ($2P_2/2P_1 = 2.2/0.14$; both numbers from Table 2), and the latter was smaller than that in liposomes made of the extracted total lipid by another factor of 2.3 ($2P/2P_2 = 5.0/2.2$; both numbers from Table 2). The exchange rates between the two domains in the viral membrane were in the range of 10^4 to 10^5 s^{-1}.

One might think that K_1 and K_2 can be determined by simply fitting the data for $A + B$ and $A - B$ in Fig. 4. However, because arbitrariness in fitting was great, it was impossible to reliably determine K_1 and K_2 in this way. Nevertheless, in future research, it may be possible to determine K_1 and K_2 by simple curve fitting because the K_1 and K_2 values determined in this work can be used as a reference guide, or the numbers may just fall in the right range to give a reliable fit.

Many biological membranes contain functional domains that are rich in integral membrane proteins (Kusumi and Hyde, 1982; Edidin, 1990; Kusumi and Sako, 1996) and cholesterol (Edidin, 1997; Brown and London, 1998; Simons and Ikonen, 1997). Nevertheless, we have a very limited understanding of molecular organization and dynamics in membranes containing high concentrations of transmembrane proteins and cholesterol (Ashikawa et al., 1994; Subczynski et al., 1998). The DOT method developed here for analysis of pulsed EPR spin label data using molecular oxygen as a probe is useful in studies of the SLOT domains, the protein-stabilized cholesterol-rich raft domains in particular, and the exchange of lipids between the SLOT domain and the BULK domain.

This work was supported in part by grants GM27665, GM22923, and RR01008 from the National Institutes of Health and by grants-in-aids from the Agency of Industrial Science and Technology of the Ministry of International Trade and Industry, and from the Ministry of Education, Science, Culture, and Sports of the Japanese government.

REFERENCES

Adams, C., and W. J. Nelson. 1998. Cytomechanics of cell adhesion structures. *Curr. Opin. Cell Biol.* 7:457–463.

Ashikawa, I., J.-J. Yin, W. K. Subczynski, T. Kouyama, J. S. Hyde, and A. Kusumi. 1994. Molecular organization and dynamics in bacteriorhodopsin-rich reconstituted membranes: discrimination of lipid environments by the oxygen transport parameter using a pulse ESR spin-labeling technique *Biochemistry.* 33:4947–4952.

Bartlett, R. G. 1959. Phosphorus assay in column chromatography. *J. Biol. Chem.* 243:466–468.

Bligh, E. G., and W. J. Dyer. 1959. A rapid method of total lipid extraction and purification. *Can. J. Biochem. Physiol.* 37:911–917.

Booy, F. P., R. W. H. Ruigrok, and E. F. J. van Bruggen. 1985. Electron microscopy of influenza virus. A comparison of negatively stained and ice-embedded particles. *J. Mol. Biol.* 184:667–676.

Brown, D. A., and E. London. 1998. Functions of lipid rafts in biological membranes. *Annu. Rev. Cell Dev. Biol.* 14:111–136.

East, J. M., D. Melville, and A. G. Lee. 1985. Exchange rates and numbers of annular lipids for the calcium and magnesium ion dependent adenosine triphosphatase. *Biochemistry.* 24:2615–2623.

Edidin, M. 1990. Molecular associations and membrane domains. *Curr. Top. Membr. Trans.* 36:81–93.

Edidin, M. 1997. Lipid microdomains in cell surface membranes. *Curr. Opin. Struct. Biol.* 7:528–532.

Edidin, M., and I. Stroynowski. 1991. Difference between the lateral organization of conventional and inositol phospholipid anchored membrane proteins. A further definition of micrometer scale membrane domains. *J. Cell Biol.* 112:1143–1150.

Field, K. A., D. Holowka, and B. Baird. 1995. Fc epsilon RI-mediated recruitment of p53/56lyn to detergent-resistant membrane domains accompanies cellular signaling. *Proc. Natl. Acad. Sci. U.S.A.* 92:9201–9.

Field, K. A., D. Holowka, and B. Baird. 1997. Compartmentalized activation of the high affinity immunoglobulin E receptor within membrane domains. *J. Biol. Chem.* 272:4276–4280.

Gaidarov, I., F. Santini, R. A. Warren, and J. H. Keen. 1998. Spatial control of coated-pit dynamics in living cells. *Nat. Cell Biol.* 1:1–7.

Ge, M., K. A. Field, R. Aneja, D. Holowka, B. Baird, and J. H. Freed. 1999. Electron spin resonance characterization of liquid ordered phase of detergent-resistant membranes from RBL-2H3 cells. *Biophys. J.* 77:925–933.

Harder, T., P. Scheiffele, P. Verkade, and K. Simons. 1998. Lipid domain structure of the plasma membrane revealed by patching of membrane components. *J. Cell Biol.* 141:929–942.

Horváth, L. I., P. J. Brophy, and D. Marsh. 1988. Exchange rates at the lipid-protein interface of myelin proteolipid protein studied by spin-label electron spin resonance. *Biochemistry.* 27:46–52.

Hwang, J., L. A. Gheber, L. Margolis, and M. Edidin. 1998. Domains in cell plasma membranes investigated by near-field scanning optical microscopy. *Biophys. J.* 74:2184–2190.

Hyde, J. S., and W. K. Subczynski. 1984. Simulation of ESR spectra of the oxygen-sensitive spin-label probe CTPO. *J. Magn. Reson.* 56:125–130.

Hyde, J. S., and W. K. Subczynski. 1989. Spin label oximetry. *In* Biological Magnetic Resonance, Vol. 8: Spin Labeling: Theory and Applications. L. J. Berliner and J. Reuben, editors. Plenum, New York. pp. 399–425.

Jacobson, K., and C. Dietrich. 1999. Looking at lipid rafts? *Trends Cell Biol.* 9:87–91.

Kanaseki, T., K. Kawasaki, M. Murata, Y. Ikeuchi, and S. Ohnishi. 1997. Structural features of membrane fusion between influenza virus and liposome as revealed by quick-freezing electron microscopy. *J. Cell Biol.* 137:1041–1056.

Kawakami, K., A. Ishihama, and M. Hamaguchi. 1981. RNA polymerase of influenza virus. I. Comparison of the virion-associated RNA polymerase activity of various strains of influenza virus. *J. Biochem.* 89: 1751–1757.

Klenk, H.-D., R. Rott, and H. Becht. 1972. On the structure of the influenza virus envelope. *Virology.* 47:579–591.

Knowles, P. F., A. Watts, and D. Marsh. 1979. Spin-label studies of lipid immobilization in dimyristoylphosphatidylcholine-substituted cytochrome oxidase. *Biochemistry.* 18:4480–4487.

Korlach, J., P. Schwille, W. W. Webb, and G. W. Feigenson. 1999. Characterization of lipid bilayer phases by confocal microscopy and fluorescence correlation spectroscopy. *Proc. Natl. Acad. Sci. U.S.A.* 96:8461–8466.

Kusumi, A., and J. S. Hyde. 1982. Spin-label saturation-transfer electron spin resonance detection of transient association of rhodopsin in reconstituted membranes. *Biochemistry.* 21:5978–5983.

Kusumi, A., and Y. Sako. 1996. Cell surface organization by the membrane skeleton. *Curr. Opin. Cell Biol.* 8:566–574.

Kusumi, A., W. K. Subczynski, and J. S. Hyde. 1982. Oxygen transport parameter in membranes as deduced by saturation recovery measurements of spin-lattice relaxation times of spin labels. *Proc. Natl. Acad. Sci. U.S.A.* 79:1854–1858.

Kusumi, A., W. K. Subczynski, M. Pasenkiewicz-Gierula, J. S. Hyde, and H. Merkle. 1986. Spin label study on phosphatidylcholine-cholesterol membranes: effect of alkyl chain length and unsaturation in the fluid phase. *Biochim. Biophys. Acta.* 854:307–317.

Lee, G. M., F. Zhang, A. Ishihara, C. L. McNeil, and K. A. Jacobson. 1993. Unconfined lateral diffusion and an estimate of pericellular matrix viscosity revealed by measuring the mobility of gold-tagged lipids. *J. Cell Biol.* 120:25–35.

Marsh, D. 1997. Stoichiometry of lipid-protein interaction and integral membrane protein structure. *Eur. Biophys. J.* 26:203–208.

Marsh, D., A. Watts, R. D. Pates, R. Uhl, P. F. Knowles, and M. Esmann. 1982. ESR spin-label studies of lipid-protein interactions in membranes. *Biophys. J.* 37:265–274.

Metzger, H. 1992. Transmembrane signaling: the joy of aggregation. *J. Immunol.* 149:1477–1487.

Miettinen, H. M., K. Matter, W. Hunziker, J. K. Rose, and I. Mellman. 1992. Fc receptor endocytosis is controlled by cytoplasmic domain determinant that actively prevents coated pit localization. *J. Cell Biol.* 116:875–888.

Mouritsen, O. G., and O. S. Andersen. 1998. In search of a new biomembrane model. *Biol. Skr. Dan. Vid. Selsk.* 49:The Royal Danish Academy of Sciences and Letters, Copenhagen.

Pasenkiewicz-Gierula, M., W. K. Subczynski, and A. Kusumi. 1991. Influences of phospholipid unsaturation on the cholesterol distribution in membranes. *Biochimie.* 73:1311–1316.

Popp, C. A., and J. S. Hyde. 1982. Electron-electron double resonance and saturation-recovery studies of nitroxide electron and nuclear spin-lattice relaxation times and Heisenberg exchange rates: lateral diffusion in dimyristoylphosphatidylcholine *Proc. Natl. Acad. Sci. U.S.A.* 79:2559–2563.

Ryba, N. J. P., L. I. Horváth, A. Watts, and D. Marsh. 1987. Molecular exchange at the lipid-rhodopsin interface: spin-label electron spin resonance studies of rhodopsin-dimyristoylphosphatidylcholine recombinants. *Biochemistry.* 26:3234–3240.

Scheiffele, P., A. Rietveld, T. Wilk, and K. Simons. 1997a. Influenza viruses select ordered lipid domains during budding from the plasma membrane. *J. Biol. Chem.* 274:2038–2044.

Scheiffele, P., M. G. Roth, and K. Simons. 1997b. Interaction of influenza virus haemagglutinin with sphingolipid-cholesterol membrane domains via its transmembrane domain. *EMBO J.* 16:5501–5508.

Simons, K., and Ikonen. 1997. Functional rafts in cell membranes. *Nature.* 387:569–572.

Singer, S. J., and G. L. Nicholson. 1972. The fluid mosaic model of the structure of cell membrane. *Science.* 175:720–731.

Sheets, E. D., Lee, G. M., Simson, R., and K. Jacobson. 1998. Transient confinement of a glycosylphosphatidylinositol-anchored protein in the plasma membrane. *Biochemistry.* 36:12449–12458.

Subczynski, W. K., W. E. Antholine, J. S. Hyde, and A. Kusumi. 1990. Micro-immiscibility and three-dimensional dynamic structure of phosphatidylcholine-cholesterol membranes: translational diffusion of copper complex in the membrane. *Biochemistry.* 29:7936–7945.

Subczynski, W. K., and J. S. Hyde. 1984. Diffusion of oxygen in water and hydrocarbons using an electron spin resonance spin label technique. *Biophys. J.* 45:743–748.

Subczynski, W. K., J. S. Hyde, and A. Kusumi. 1989. Oxygen permeability of phosphatidylcholine-cholesterol membranes. *Proc. Natl. Acad. Sci. U.S.A.* 86:4474–4478.

Subczynski, W. K., J. S. Hyde, and A. Kusumi. 1991. Effect of alkyl chain unsaturation and cholesterol intercalation on oxygen transport in membranes: a pulse ESR spin labeling study. *Biochemistry.* 30:8578–8590.

Subczynski, W. K., R. N. A. H. Lewis, R. N. McElhaney, R. S. Hodges, J. S. Hyde, and A. Kusumi. 1998. Molecular organization and dynamics of 1-palmitoyl-2-oleoyl-phosphatidylcholine bilayers containing a transmembrane α-helical peptide. *Biochemistry.* 37:3156–3164.

Subczynski, W. K., G. Renk, R. Crouch, J. S. Hyde, and A. Kusumi. 1992. Oxygen diffusion-concentration product in rhodopsin as observed by a pulse ESR spin labeling method. *Biophys. J.* 63:573–577.

Subczynski, W. K., A. Wisniewska, J.-J. Yin, J. S. Hyde, and A. Kusumi. 1994. Hydrophobic barriers of lipid bilayer membranes formed by reduction of water penetration by alkyl chain unsaturation and cholesterol. *Biochemistry.* 33:7670–7681.

Thomas, J. L., D. Holowka, B. Baird, and W. W. Webb. 1994. Large-scale co-aggregation of fluorescent lipid probes with cell surface proteins. *J. Cell Biol.* 125:795–802.

Torigoe, C., J. K. Inman, and H. Metzger. 1998. An unusual mechanism for ligand antagonism. *Science.* 281:568–572.

Varghese, J. N., W. G. Laver, and P. M. Colman. 1983. Structure of the influenza virus glycoprotein antigen neuraminidase at 2.9 Å resolution. *Nature.* 303:35–40.

Webster, R. G., W. G. Laver, G. M. Air, and G. C. Schild. 1982. Molecular mechanisms of variation in influenza viruses. *Nature.* 296:115–121.

Wilson, I. A., J. J. Skehel, and D. C. Wiley. 1981. Structure of the haemagglutinin membrane glycoprotein of influenza virus at 3 Å resolution. *Nature.* 289:366–378.

Windrem, D. A., and W. Z. Plachy. 1980. The diffusion-solubility of oxygen in lipid bilayers. *Biochim. Biophys. Acta.* 600:655–665.

Yin, J.-J., J. B. Feix, and J. S. Hyde. 1988. Solution of the nitroxide spin-label spectral overlap problem using pulse electron spin resonance. *Biophys. J.* 53:523–531.

Yin, J.-J., J. B. Feix, and J. S. Hyde. 1990. Mapping of collision frequencies for stearic acid spin labels by saturation-recovery electron paramagnetic resonance. *Biophys. J.* 58:713–720.

Yin, J.-J., M. Pasenkiewicz-Gierula, and J. S. Hyde. 1987. Lateral diffusion of lipid in membranes by pulse saturation recovery electron spin resonance. *Proc. Natl. Acad. Sci. U.S.A.* 84:964–968.